European Review for Medical and Pharmacological Sciences 2012; 16: 2021-2028

The use of high resolution magnetic resonance on 3.0-T system in the diagnosis and surgical planning of intraosseous lesions of the jaws: preliminary results of a retrospective study

M. CASSETTA, S. DI CARLO, N. PRANNO, A. STAGNITTI*, V. POMPA, G. POMPA

Department of Oral and Maxillofacial Sciences, School of Dentistry, Sapienza University of Rome, Rome, Italy
*Department of Radiological Sciences, Sapienza University of Rome, Rome, Italy

Abstract. – BACKGROUND: The pre-operative evaluation in oral and maxillofacial surgery is currently performed by computerized tomography (CT). However in some case the information of the traditional imaging methods are not enough in the diagnosis and surgical planning. The efficacy of these imaging methods in the evaluation of soft tissues is lower than magnetic resonance imaging (MRI).

AIM: The aim of the study was to show the use of MRI in the evaluation of relation between intraosseous lesions of the jaws and anatomical structures, when it was difficult using the traditional radiographic methods, and to evaluate the usefulness of MRI to depict the morphostructural characterization of the lesions and infiltration of the soft tissues.

MATERIALS AND METHODS: 10 patients with a lesion of jaw were selected. All the patients underwent panoramic radiography (OPT), CT and MRI. The images were examined by dental and maxillofacial radiology who compared the different imaging methods to analyze the morphological and structural characteristics of the lesion and assessed the relationship between the lesion and the anatomical structures.

RESULTS: Magnetic resonance imaging provided more detailed spatial and structural information than other imaging methods.

CONCLUSIONS: MRI allowed us to characterize the intraosseous lesions of the jaws and to plan the surgery, resulting in a lower risk of anatomic structures surgical injury.

Key Words:
Odontogenic tumours, Odontogenic cysts, Mandibular nerve, Tomography X-Ray computed, Magnetic resonance imaging.

Introduction

Benign odontogenic tumours and cysts are asymptomatic intraosseous lesion that can affect the bones of the maxillomandibular complex. Ameloblastomas and keratocystic odontogenic tumours are major aggressive odontogenic tumours[1]. These tumours are characterized by a low speed expansion and they are frequently associated to a local invasion of the contiguous epithelial areas[2]. Both tumours show more frequently a localization at the angle of the mandible, extending anteriorly and superiorly, and common radiologic features such as unilocular or multilocular radiolucencies with a characteristic "soap bubble" shape[2]. A radiological differentiation between ameloblastomas and keratocystic odontogenic tumours lesions is not difficult if the lesions show their characteristic aspect. However, some time, these tumours appear as unilocular and the differential diagnosis with the other damages is difficult. The pre-operative evaluation in oral and maxillofacial surgery is currently performed by several imaging methods. One of the principal difficulties in the planning of surgery is to define the anatomic relation between the lesion and peripheral nerves. In particular, the evaluation of the spatial relationship between the inferior alveolar nerve (IAN) and a mandibular lesion is important to avoid injuries of this anatomic structure[3-5].

Both panoramic radiography (OPT) and computerized tomography (CT) can be used to detect the bone structures. However, the efficacy of these imaging methods in the IAN detection is lower than magnetic resonance imaging (MRI). In fact, while CT and OPT depict the bone of the mandibular canal, MRI allows a significant appreciation of its contents[6-9].

Matsuzaki et al[10] also showed the utility of the MRI in the pre-surgical approach, especially in the evaluation of soft tissue invasion in ameloblastic carcinoma in the right anterior maxillary sinus.

Corresponding Author: Michele Cassetta, DDS, Ph.D.; e-mail: michele.cassetta@uniroma1.it

The aim of the present study was to show the use of MRI in the evaluation of relation between intraosseous lesions of the jaws and the anatomical structures, when it was difficult using the traditional radiographic methods, and to evaluate the usefulness of MRI to depict the morphostructural characterization of these lesions and infiltration of the soft tissues.

Materials and Methods

Patient Population

A total of 10 patients, six men and four women (age range: 21-63 years; means: 38.8 years), who had a lesion of jaws, were selected at the Department of Oral and Maxillofacial Sciences of "Sapienza" University of Rome (Table I). All patients, between January 2004 and April 2010, underwent OPT, CT and MRI to provide a careful morphostructural characterization and evaluation of spatial relationship between the lesion and the anatomic structures. All images were analyzed by dental and maxillofacial radiologist.

CT Imaging

CT examinations were performed in high resolution helical CT machines (CT scan Siemens Somatom, Erlangen, Germany) using a bone algorithm, 0.6 mm slice collimation, 24 cm field of View (FOV), 512 × 512 matrix, 120 kV and 150 mAs. The data were transferred to the workstation for post-processing. Three sets of reconstruction images were displayed: Axial, Sagittal and Coronal.

MR Imaging

MRI scan with a 3.0 T machine (Discovery 750 General Electric, Milwaukee, WI, USA) was performed with head-neck coil. Since the maxillofacial area is composed by a high percentage of fat and fluid, the study of this region could not be performed by means of routine conventional techniques of MRI. Consequently, our protocol was carried out using the following sequences:

1. T2-weighted axial images acquired with a fast spin echo interactive decomposition of water and fat with echo asymmetry and least-squares estimation (FSE IDEAL) using a repetition time (TR) of 3038 ms, echo time (TE) of 124 ms, field of view (FOV) of 24 × 24 cm, slice-thickness (SL) of 4 mm, and number of excitations (NEX) of 3.
2. T1-weighted axial images fat-saturated fast spin echo pre-contrast administration (Ax T1 Fs FSE pre-CE) and post-contrast administration (Ax T1 Fs FSE post-CE) using a repetition time (TR) of 418 ms, echo time (TE) of 8 ms, field of view (FOV) of 25 × 25 cm, slice-thickness (SL) of 4 mm, and number of excitations (NEX) of 2 to evaluate the potential enhancement of the mass.
   The contrast index (CI) pre- and post-contrast administration was calculated using one region of interest (ROI) in the centre of the tumour mass (a ROI in the muscular tissue was used as a control-image). Contrast-enhanced MRI (CE-MRI) with gadoteric acid (Dotarem, 12 ml) was performed to evaluate possible soft tissue invasion and to investigate the benign nature of the lesion.
3. Diffusion weighted imaging (DWI b = 800) using a repetition time (TR) of 4375 ms, echo time (TE) of 72 ms, field of view (FOV) of 23 × 23 cm, slice-thickness (SL) of 5 mm, bandwidth (b) of 800 s/mm^2 and number of excitations (NEX) of 1.
4. T1-weighted fast imaging employing steady-state acquisition (FIESTA) using a repetition time (TR) of 4.6 ms, echo time (TE) of 2.2 ms, field of view (FOV) of 24 × 24 cm, slice-thickness (SL) of 0.6 mm and number of excitations (NEX) of 1 and T1-weighted fast spoiled gradient-recalled echo (fast SPGR) using a repetition time (TR) of 7.8 ms, echo time (TE) of 3.2 ms, field of view (FOV) of 23.5 × 23.5 cm, slice-thickness (SL) of 0.6 mm and number of excitations (NEX) of 2.

For the criteria of the signal intensity the cerebrospinal fluid was defined as a bright hight signal on T2WI and muscolature as a intermediate signal on T1WI.

Results

This study included 10 patients. The histological diagnosis was dentigerous cysts in 8 patients, unicystic ameloblastoma in 1 patient and solid/multicystic ameloblastoma in 1 patient (Table I).

In the Water: (T2 FSE-IDEAL) the odontogenic cyst and unicystic ameloblastoma appeared as a homogeneously high signal intensity region, and it was characterized by homogeneously intermedial intensity in the Fat: (T2 FSE-IDEAL).

Otherwise ameloblastoma solid/multicystic appeared as a high signal intensity region in the

Table I. Clinical and MR imaging features.

	Age	Sex	Region	T1-weighted image	Water T2-weighted image	Fat T2-weighted image	Contrast-enhanced T1-weighted image	Histopathological diagnosis
1	27	F	Left maxillary region	Homogeneously intermediate	Homogeneously high	Homogeneously intermediate	Thin rim enhancement	Odontogenic cysts
2	63	F	Maxillary anterior region	Homogeneously intermediate	Homogeneously high	Homogeneously intermediate	Thin rim enhancement	Odontogenic cysts
3	35	M	Left mandibular ramus	Homogeneously intermediate	Homogeneously bright high	Homogeneously intermediate	Thick rim enhancement	Unicystic type of ameloblastoma
4	45	F	Left mandibular ramus	Homogeneously intermediate	Homogeneously high	Homogeneously intermediate	Thin rim enhancement	Odontogenic cysts
5	43	M	Left mandibular ramus	Intermedial (cystic portion) Intermediate (solid portion)	Bright high (cystic portion) High (solid portion)	High (cystic portion) High-intermedial (solid portion)	No enhancement (cystic portion) Good enhancement (solid portion)	Solid/multicystic type of ameloblastoma
6	31	M	Right mandibular ramus	Homogeneously intermediate	Homogeneously high	Homogeneously intermediate	–	Odontogenic cysts
7	52	M	Right mandibular molar	Homogeneously intermediate	Homogeneously high	Homogeneously intermediate	Thin rim enhancement	Odontogenic cysts
8	21	F	Left maxillary region	Homogeneously intermediate	Homogeneously high	Homogeneously intermediate	–	Odontogenic cysts
9	23	M	Right mandibular ramus	Homogeneously intermediate	Homogeneously high	Homogeneously intermediate	Thin rim enhancement	Odontogenic cysts
10	48	M	Left mandibular ramus	Homogeneously intermediate	Homogeneously high	Homogeneously intermediate	Thin rim enhancement	Odontogenic cysts

Water: (T2 FSE-IDEAL) and it was characterized by hight-intermedial intensity in the Fat: (T2 FSE-IDEAL). Both the sequences unveiled an heterogeneous pattern within the tumour mass (Figure 1).

Ax T1 Fs FSE pre-CE in the odontogenic cyst and unilocular cystic-type ameloblastomas showed homogeneous intermediate signal intensity. In the solid/multicistic ameloblastomas Ax T1 Fs FSE pre-CE showed intermedial signal intensity in cystic and solid portion.

Ax T1 Fs FSE post-CE in the odontogenic cyst and unilocular cystic-type ameloblastomas showed a thick or thin rim enhancement. In the solid/multicistic ameloblastomas Ax T1 Fs FSE post-CE showed an area of solid component characterizad by a good enhancement.

No significant differences were observed in the CI between the two ROIs in the lesions (Figure 2).

The DWI sequence showed in three patients hypointense lymph nodes, increased in size, ipsilateral to the lesion (Figure 3).

3D FIESTA and fast-SPGR are both three dimensional sequences that visualize directly the reciprocal relationship between the anatomic and pathological structures, in particular is possible to assess the IAN course. In the 100% of the cases we were capable to value the spatial relation between the lesions and the anatomical structures using the 3D FIESTA and SPGR scan (Figure 4).

CT scans in all patients detected the bone structures providing an high spatial resolution.

However, in two cases, when the lesion induced the resorption of the roof of the mandibular canal, the IAN could not be identified by CT (Figure 4).

Discussion

MRI images of intraosseous lesions of the jaws provided additional information compared to CT in the several sequences that have been used in the present study.

The IDEAL sequence allowed to acquire 3 images with different phase shifts between water and fat saturation thus leading to the possibility to distinguish water and fat images and the field map. In order to obtain this separation, iterative fat-water decomposition algorithm and a 3-echo data acquisition, with the center echo shifted relative to the SE point, were combined. This sequence allowed to depict the component (solid or liquid) of the lesion. On this T2-weighted images (T2WI) the signal intensity of a lesion was designated as homogeneously high or intermedial in the odontogenic cyst and unilocular cystic-type ameloblastomas. Otherwise, ameloblastoma solid/multicystic appeared as a high or intermedial signal intensity region. On T1-weighted images (T1WI) odontogenic cyst and unilocular cystic-type ameloblastomas were designated as homogeneous intermediate signal intensity area. The solid/multicistic ameloblastomas showed intermedial signal intensity in cystic and solid por-

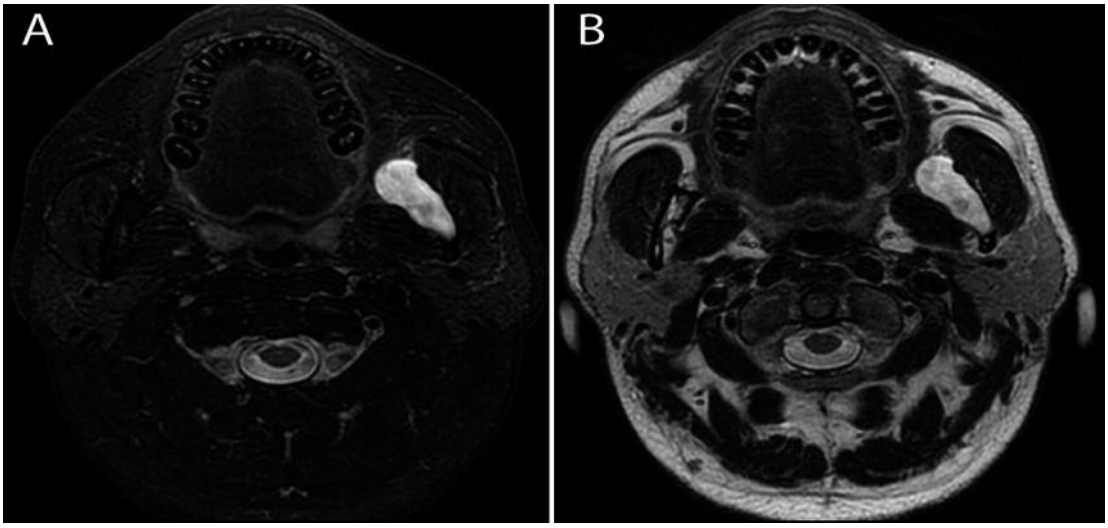

Figure 1. T2-weighted axial images acquired with a fast spin echo interactive decomposition of water and fat with echo asymmetry and least-squares estimation (FSE IDEAL). Water ***(A)*** and Fat ***(B)*** (T2 FSE-IDEAL) show an heterogeneous pattern within the solid/multicistic ameloblastomas tumour mass.

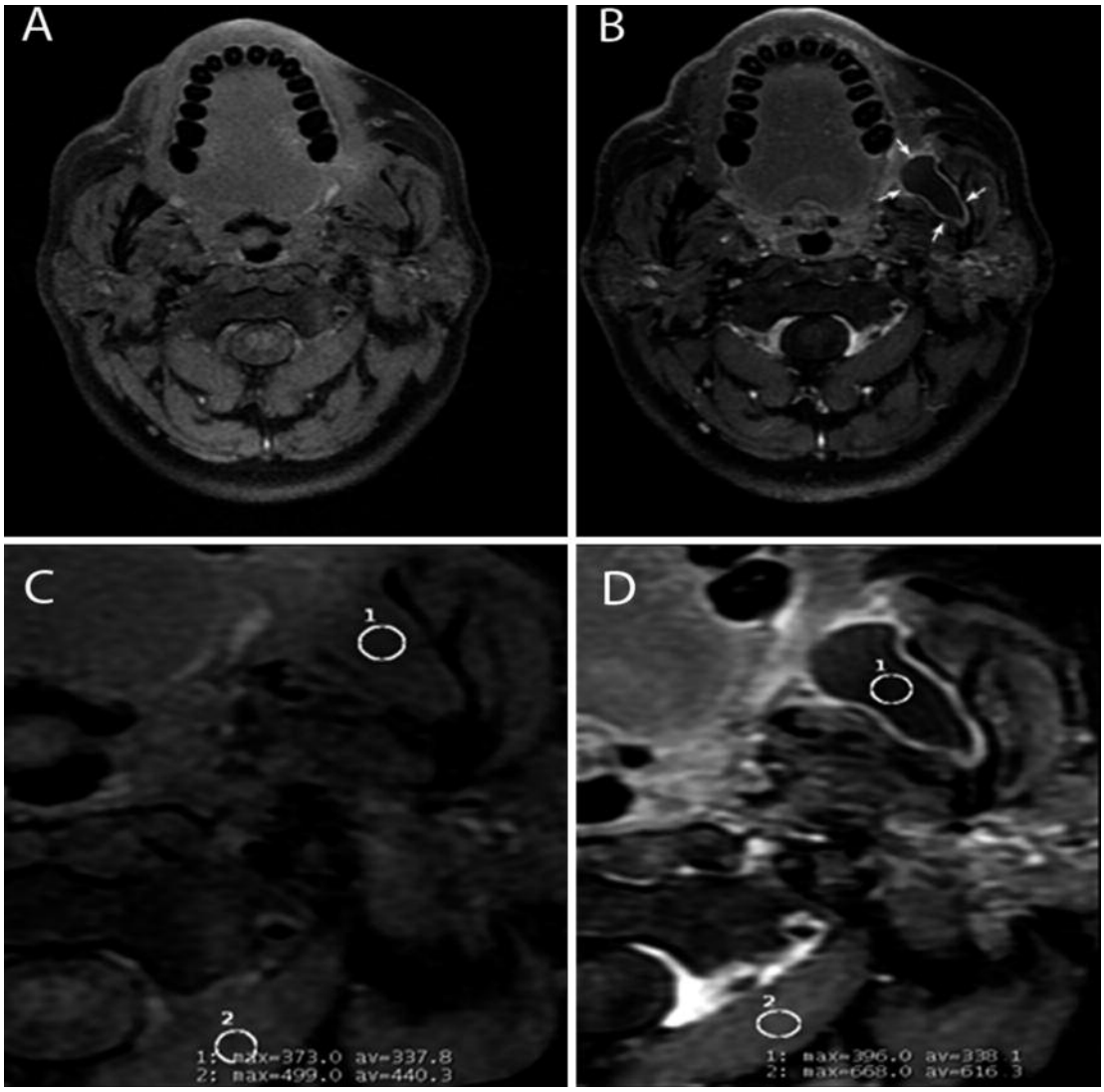

Figure 2. T1-weighted axial images fat-saturated fast spin echo (Ax T1 Fs FSE). ***A,*** Pre-contrast administration (Ax T1 Fs FSE pre-CE). ***B,*** Post-contrast administration (Ax T1 Fs FSE post-CE). The post-CE acquisition shows that the contrast is confined to the margin of the lesion,characteristic image of the benign tumour with the presence of a capsule. Two ROIs corresponding to the lesion (1) and to the muscular tissue (2) were determined in the pre ***(C)*** and post-contrast administration ***(D)*** sequences. A significant different gradient between the two sequences was detected only in the muscular tissue. Consequently no mass enhancement was observed.

tion. The characteristic heterogeneous pattern within this tumour mass was due to his multicystic and solid structure. Otherwise, homogeneously hight/intermedial signal intensity on T2WI and homogeneously intermediate signal intensity on T1WI reflected the fluid content of the inner part of odontogenic cyst and unilocular cystic-type ameloblastomas. T1WI post-contrast administration revealed an encapsulated lesion and highlighted well defined margins. This finding allowed us to assign the diagnosis of a benign lesion. In all lesions CE-MRI showed a bright high rim signal intensity. The only patient with the unicystic ameloblastoma was characterize by more thick rim enhancement useful for the differentiation of unilocular cystic-type ameloblastoma from other cystic lesions. CE-MRI demonstrated that the solid/multicystic ameloblastomas were composed of varying proportion of solid (good enhancement) and cystic (no enhancement) lesions useful in the differential diagnosis with the other intraosseous tumours. In all lesions two ROIs corresponding to the lesion and to the muscular tissue were determined in the pre and post-contrast administration sequences. No significant gradient differences between the two sequences

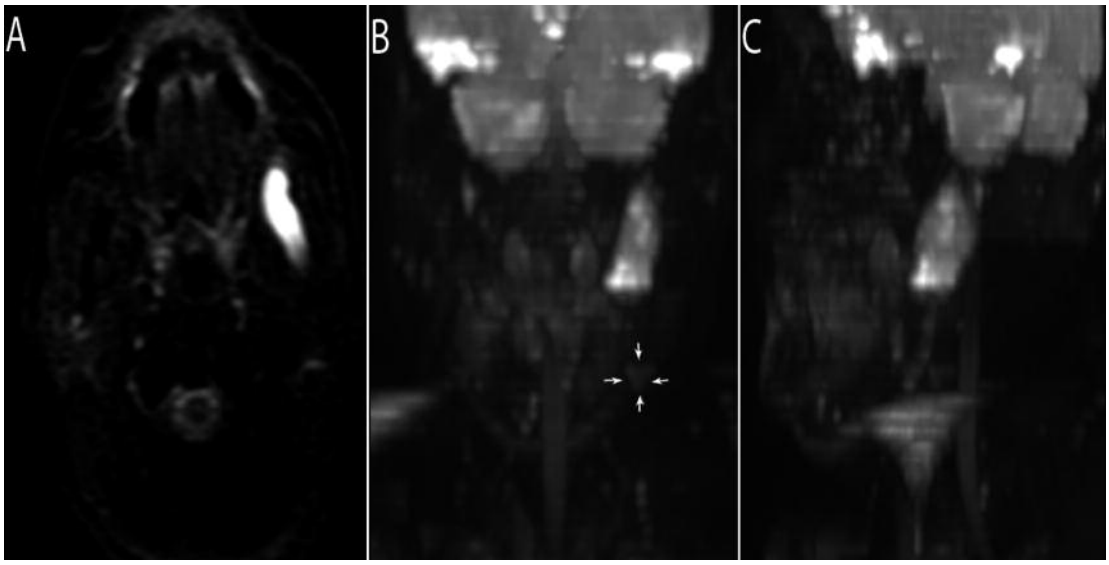

Figure 3. Diffusion weighted imaging acquisition (DWI b = 800): ***A,*** Axial diffusion-weighted MR image at b = 800 s/mm^2 shows an high signal intensity of the lesion. ***B-C,*** High resolution 3D Volume Rendering 3DVR-MRI shows enlarged nodes, ipsilateral to the lesion, in the upper part of the neck which exhibit low signal intensity. The white arrows indicate an enlarged node.

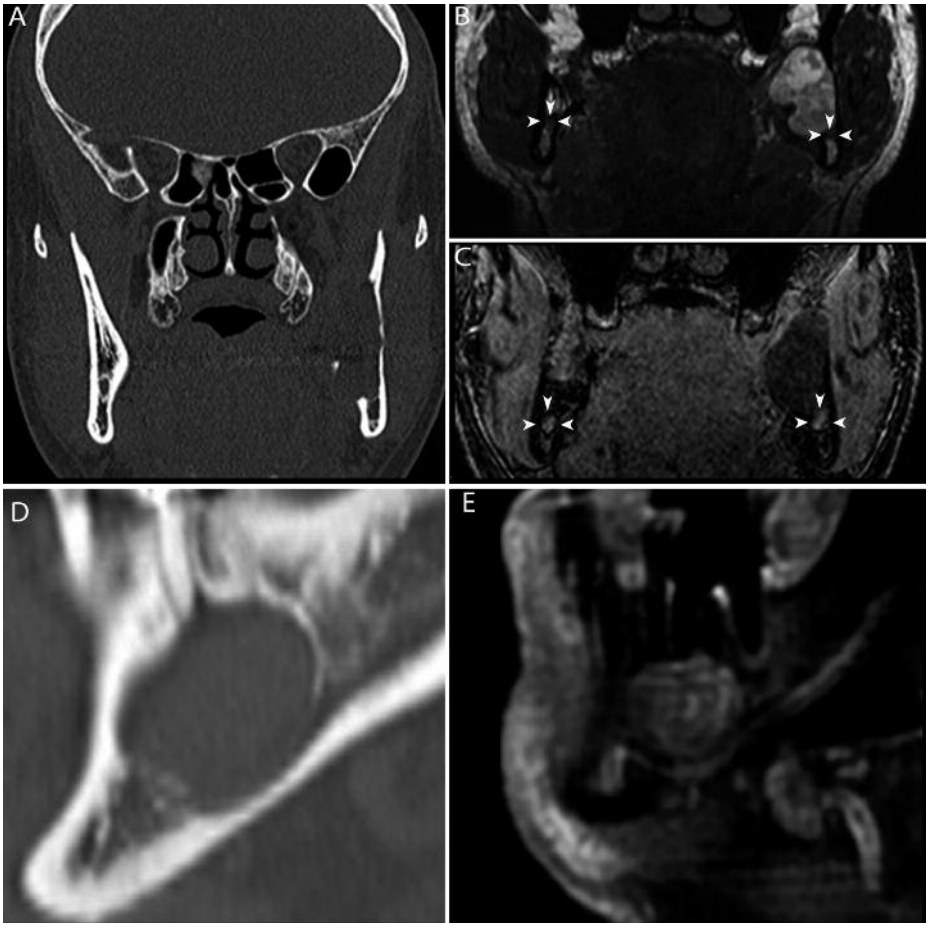

Figure 4. Coronal CT image of the patient with solid/multicystic ameloblastoma in the left mandible ramus ***(A)*** the relationship between the lesion and the mandibular canal is not detectable; in the coronal T1-weighted fast imaging employing steady-state acquisition (FIESTA) ***(B)*** and in the coronal T1-weighted fast spoiled gradient-recalled echo (fast SPGR) ***(C)*** the relationship between the lesion and IAN (white arrows) is clearly detectable. Sagittal CT image of the patient with unilocular odontogenic cyst in the right mandibular molar area ***(D)*** the relationship between the lesion and the mandibular canal is not detectable; In the sagittal T1-weighted axial images fat-saturated fast spin echo post-contrast administration (Ax T1 Fs FSE post-CE) ***(E)*** the relationship between the lesion and IAN is clearly detectable.

were observed. Consequently no mass enhancement were observed and in all cases the infiltrations of soft tissue were negative[10-12].

DWI was applied for the evaluation of intracranial diseases such as cerebrovascular accidents, trauma and epilepsy diseases such. Currently, DWI (diffusion weighted imaging) is being used for tumour detection, tumour characterisation and to differentiate neoplastic from non-neoplastic diseases, and is being employed in various organ systems. This sequence evaluates intercellular water motion: every change in the water protons movements induces a variation of signal intensity in this sequence[13]. DWI is currently used to improve the diagnostic accuracy in the differential diagnosis between benign and malignant nodes. Metastatic nodes are characterized by reduction of diffusivity, which is associated with a hypercellularity, to an increased nuclear-to-cytoplasmatic ratio and to perfusion. This decrement in diffusion is represented as an area of hyperintensity on diffusion images; adversely, inflammatory nodes appeared hypointense[14]. In this study the DWI sequence showed in three cases a benign latero-cervical lymphadenopathy, ipsilateral to the lesion. No malignant lymph nodes were observed.

3D FIESTA and fast-SPGRT used in the present study are both high reliable to provide a precise estimation of spatial relation between the lesions and the anatomic structures supplementing clear anatomical visualization. In particular, the 3-D FIESTA is a T2 weighted sequence widely used for the study of the intracranial path of the cranial nerves, as it performs a "cisternography" inside the skull and it is used in the clinical practice to rule out the presence of the acoustic neurinoma in the clinical suspicion of hearing loss of neurosensory type[15,16]. The 3D FIESTA allows also to follow the fifth cranial nerve, especially in his third and main branch (the mandibular nerve) It is also possible to follow the inferior alveolar nerve and the lingual nerve, frequently interested by intraosseous expansive lesions, being these two nerves the main branches of the posterior trunk of the mandibular nerve.

The fast SPGR sequence is a T1 sequence fat sat, giving an high contrast between the bone of the jaw and the alveolar nerve that appear as hyper-intense inside the bone itself. Despite the low discrimination between the soft tissues the fast SPGR (spoiled gradient-recalled) gives a very reliable and good quality of image of the inferior alveolar nerve, allowing to assess its path directly[17]. In the 100% of the cases we were capable to value the spatial relation between the lesions and the anatomical structures with the 3D FIESTA and SPGR scan.

CT plays an important role in the study of intraosseous lesions and in the evaluation of adjacent bone destruction[18]. The ability of this x-ray method to eliminate image superimposition, to present real dimensional values, to reconstruct high resolution images in different planes including 3 dimensions, has established CT as the gold standard in diagnosis and treatment planning of this lesions[19,20]. In this study it revealed, in the cases of odontogenic cyst and unilocular cystic-type ameloblastomas, a unilocular radiolucency, variable in size, presenting well defined margins. In the case of ameloblastoma solid/multicystic CT showed multiple-locus radiolucency presenting characteristic "soap bubble" shape, interesting the whole left mandibular ramus. CT scans in all patients detected the bone structures providing an high spatial resolution. However, in two cases, when the lesion induced the resorption of the roof of the mandibular canal CT imaging has provided unclear depiction of the mandibular canal. In contrast, the present MRI protocol provided high resolution images of these anatomic structures and it was decisive for the surgical planning, reducing the risk of IAN damage.

Conclusions

MRI has been infrequently used for oral and maxillofacial imaging because the acquisition of the sequences can be invalidated by motion of the body, respiration, air in the oral cavity and nasal cells, implants and metal materials[3,21]. However, the utilization of MRI, allowed us a careful evaluation of spatial relationship between anatomic structures and intraosseous jaws lesions when CT imaging has provided unclear depiction of the mandibular canal. The actual study showed that MRI could be effectively useful to the typing of different expansive lesion, and to evaluate the possible infiltration of the soft tissue. These informations are decisive in the differential diagnosis between the benign lesions and major aggressive odontogenic tumours and in the surgical planning. Therefore, the capability to acquire more news without exposing the patient to x-rays makes the MRI an additional imaging method in oral and maxillofacial surgery[22].

However, the results of this study should be interpreted taking into account the limited number of cases and further evaluations will be done when will be available a wider number of cases.

References

1) Cassetta M, Tarantino F, Calasso S. Conservative treatment of odontogenic keratocyst: a case report and review of the literature. Dental Cadmos 2009; 77: 19-40.
2) Barnes L, Eveson JW, Reichart P, Sidransky D. World Health Organization classification of tumours: pathology and genetics of head and neck tumours. Lyon: International Agency for Research on Cancer Press, 2005.
3) Seo K, Terumistu M, Tanaka Y, Tsurumaki T, Kurata S, Matsuzawa H, Takagi R. Preoperative evaluation of spatial relationship between inferior alveolar nerve and Fibro-osseous lesion by high resolution magnetic resonance neurography on 3.0-T system: a case report. J Oral Maxillofac Surg 2012; 70: 119-123.
4) Filler AG, Howe FA, Hayes CE, Kliot M, Winn HR, Bell BA, Griffiths JR, Tsuruda JS. Magnetic resonance neurography. Lancet 1993; 341: 659-661.
5) Filler AG, Kliot M, Howe FA, Hayes CE, Saunders DE, Goodkin R, Bell BA, Winn HR, Griffiths JR, Tsuruda JS. Application of magnetic resonance neurography in the evaluation of patients with peripheral nerve pathology. J Neurosurg 1996; 85: 299-309.
6) Wei D, Song-Ling C, Zhong-Wei Z, Dai-Ying H, Xing Z, Xiang L. High-resolution magnetic resonance imaging of the inferior alveolar nerve using 3-dimensional magnetization-prepared rapid gradient-echo sequence at 3.0T. J Oral Maxillofac Surg 2008; 66: 2621-2626.
7) Ikeda K, Ho KC, Nowicki BH, Haughton VM. Multiplanar MR and anatomic study of the mandibular canal. Am J Neuroradiol 1996; 17: 579-584.
8) Nasel CJ, Pretterklieber M, Gahleitner A, Czerny C, Breitenseher M, Imhof H. Osteometry of the mandible performed using dental MR imaging. Am J Neuroradiol 1999; 20: 1221-1227.
9) Eggers G, Rieker M, Fiebach J, Kress B, Dickhaus H, Hassfeld S. Geometric accuracy of magnetic resonance imaging of the mandibular nerve. Dentomaxillofac Radiol 2005; 34: 285-291.
10) Matsuzaki H, Katase N, Hara M, Asaumi J, Yanagi Y, Unetsubo T, Hisatomi M, Konouchi H, Nagatsuka H. Ameloblastic carcinoma: a case report with radiological features of computed tomography and magnetic resonance imaging and positron emission tomography. Oral Surg Oral Med Oral Pathol Oral Radiol Endod 2011; 112: 40-47.
11) Hisatomi M, Yanagi Y, Konouchi H, Matsuzaki H, Takenobu T, Unetsubo T, Asaumi J. Diagnostic value of dynamic contrast-enhanced MRI for unilocular cystic-type ameloblastomas with homogeneously bright high signal intensity on T2-weighted or STI MR images. Oral Oncol 2011; 47: 147-152.
12) Minami M, Kaneda T, Ozawa K, Yamamoto H, Itai Y, Ozawa M, Yoshikawa K, Sasaki Y. Cystic lesions of the maxillomandibular ragion: MR imaging distinction of odontogenic keratocysts and ameloblastomas from other cysts. Am J Roentgenol 1996; 166: 943-949.
13) Rowley H, Grant E, Roberts T. Diffusion MR imaging. Theory and application. Neuroimaging Clin N Am 1999; 9: 343-361.
14) Perrone A, Guerrisi P, Izzo L, D'Angeli I, Sassi S, Mele LL, Marini M, Mazza D, Marini M. Diffusion-weighted MRI in cervical lymph nodes: differentiation between benign and malignant lesions. Eur J Radiol 2011; 77: 281-286.
15) Hatipo lu HG, Durako lugil T, Ciliz D, Yüksel E. Comparison of FSE T2W and 3D FIESTA sequences in the evaluation of posterior fossa cranial nerves with MR cisternography. Diagn Interv Radiol 2007; 13: 56-60.
16) Okumura Y, Suzuki M, Takemura A, Tsujii H, Kawahara K, Matsuura Y, Takada T. [Visualization of the lower cranial nerves by 3D-FIESTA]. Nihon Hoshasen Gijutsu Gakkai Zasshi 2005; 61: 291-297.
17) Terumitsu M, Seo K, Matsuzawa H, Yamazaki M, Kwee IL, Nakada T. Morphologic evaluation of the inferior alveolar nerve in patients with sensory disorders by high-resolution 3D volume rendering magnetic resonance neurography on a 3.0-Tsystem. Oral Surg Oral Med Oral Pathol Oral Radiol Endod 2011; 111: 95-102.
18) Valentini V, Terenzi V, Cassoni A, Bosco S, Brauner E, Shahinas J, Pompa G. Giant cell lesion or Langerhan's cell histiocytosis of the mandible? A case report. Eur J Inflammation 2012; 10: 159-164.
19) Cassetta M, Stefanelli LV, Di Carlo S, Pompa G, Barbato E. The accuracy of CBCT in measuring jaws bone density. Eur Rev Med Pharmacol Sci 2012; 16: 1425-1429.
20) Cassetta M, Pompa G, Di Carlo S, Piccoli L, Pacifici A, Pacifici L. The influence of smoking and surgical technique on the accuracy of mucosa-supported stereolithographic surgical guide in complete edentulous upper jaws. Eur Rev Med Pharmacol Sci 2012; 16: 1546-1553.
21) Hubálková H, La Serna P, Linetskiy I, Dostálová T. Dental alloys and magnetic resonance imaging. Int Dent J 2006; 56: 135-141.
22) Mazza D, Marini M, Impara L, Cassetta M, Scarpato P, Barchetti F, Di Paolo C. Anatomic examination of the upper head of the lateral pterygoid muscle using magnetic resonance imaging and clinical data. J Craniofac Surg 2009; 20: 1508-1511.